BIOCHEMISTRY
including biophysical chemistry & molecular biology

Article

pubs.acs.org/biochemistry

Structural and Functional Analysis of Angucycline C-6 Ketoreductase LanV Involved in Landomycin Biosynthesis

Pasi Paananen, Pekka Patrikainen, Pauli Kallio, Pekka Mäntsälä, Jarmo Niemi, Laila Niiranen, and Mikko Metsä-Ketelä*

Department of Biochemistry and Food Chemistry, University of Turku, FIN-20014 Turku, Finland

Supporting Information

ABSTRACT: Angucyclines are biologically active natural products constructed around a common benz[*a*]-anthraquinone carbon frame. One key branching point in the biosynthesis of angucyclines is the ketoreduction at C-6, which results in the opposite stereochemistry of landomycins and urdamycins/gaudimycins. Here we present the 1.65 Å resolution crystal structure of LanV from *Streptomyces cyanogenus* S136 that is responsible for the 6*R* stereochemistry of landomycins. The enzyme displays the common architectural fold of short-chain alcohol dehydrogenases/reductases and contains bound nicotinamide adenine dinucleotide phosphate. Determination of the structure of LanV in complex with 11-deoxylandomycinone at 2.0 Å resolution indicated that substrate binding does not induce large conformational changes and that substrate recognition occurs mainly through hydrophobic interactions. Analysis of the electron density map of the ternary complex revealed that the catalytic reaction had most likely proceeded backward in the crystal, because the data could be best fit with a compound harboring a carbonyl group at C-6. A coordinated water molecule was atypically identified between the ligand and the conserved Tyr160 residue, which was confirmed to be critical for the catalytic activity by site-directed mutagenesis. A catalytic triad of Ser147, Tyr160, and Lys164 could be recognized on the basis of the crystal structure, and stereoselective labeling studies demonstrated that the transfer of hydride from reduced nicotinamide adenine dinucleotide phosphate to the substrate occurs from the 4-*pro*-*S* side of the cosubstrate. Importantly, Ser192 was identified as being involved in controlling the stereochemistry of the reaction, as assays with single mutant Ser192Ile led to accumulation of gaudimycin C with 6*S* stereochemistry as a minor product.

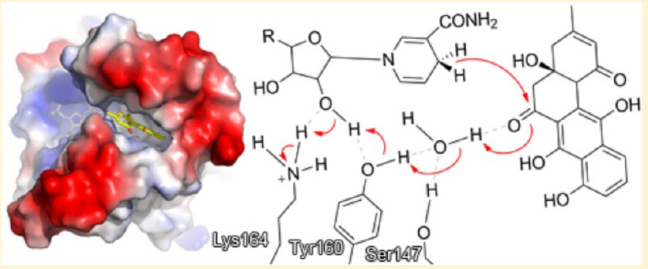

Bacteria of the genus *Streptomyces* have been a rich source of biologically active natural products, many of which have found applications in medicine and agriculture.[1] Over the years, aromatic type II polyketides, which make up a distinct subclass of bacterial secondary metabolites, have been extensively used as antibiotics (e.g., tetracycline)[2] and in cancer chemotherapy (e.g., doxorubicin).[3] Angucyclines form one large and important family of aromatic polyketides that also harbor significant biological activities.[4−6] Compounds such as landomycins,[7] urdamycins,[8] and gaudimycins[9] consist of a polyketide-derived tetracyclic benz[*a*]anthraquinone carbon skeleton onto which deoxysugar moieties may be attached via an O- or C-glycosidic linkage (Scheme 1A). The landomycins in particular have received a great deal of attention because of their notable antitumor activities and the fact that the compounds are not transported outside of cells by multidrug resistance efflux pumps,[10] which is in contrast to several other anticancer drugs currently in clinical use (e.g., doxorubicin). The exact mode of action of landomycins has remained elusive, but it has been suggested that landomycins interfere with enzymes involved in DNA synthesis or repair.[11]

Angucyclines are biologically synthesized via dedicated pathways, which may contain as many as 20−30 individual enzymatic steps.[6,12] Early stages of the biosynthesis shared by all angucyclic metabolites involve the formation of a long polyketide chain through repeated Claisen condensations of malonyl-CoA units by the minimal polyketide synthase (PKS) machinery. The highly reactive polyketide is tethered to an acyl carrier protein (ACP) during the synthesis, and the characteristic angular shape of the compounds is obtained through controlled reductions, aromatizations, and cyclizations.[13] The reduction of the carbonyl group at C-9 of the polyketide has been extensively investigated on the actinorhodin and hedamycin pathways, where the studies have indicated that the short-chain alcohol dehydrogenases/reductases (SDRs) ActKR and HedKR utilize ACP-bound bicyclic intermediates as substrates.[14,15] Finally, the fully processed polyketide is released from the ACP, and the first stable intermediate of many angucycline pathways, prejadomycin, is formed.[16]

Our recent focus has been on post-PKS tailoring reactions, which are responsible for further modification of prejadomycin. Together with variable glycosylation patterns, the alternative

Received: June 6, 2013
Revised: July 10, 2013
Published: July 12, 2013

dx.doi.org/10.1021/bi400712q | *Biochemistry* 2013, 52, 5304−5314

Scheme 1. Angucycline Antibiotics and Early Tailoring Steps in Their Biosynthesis[a]

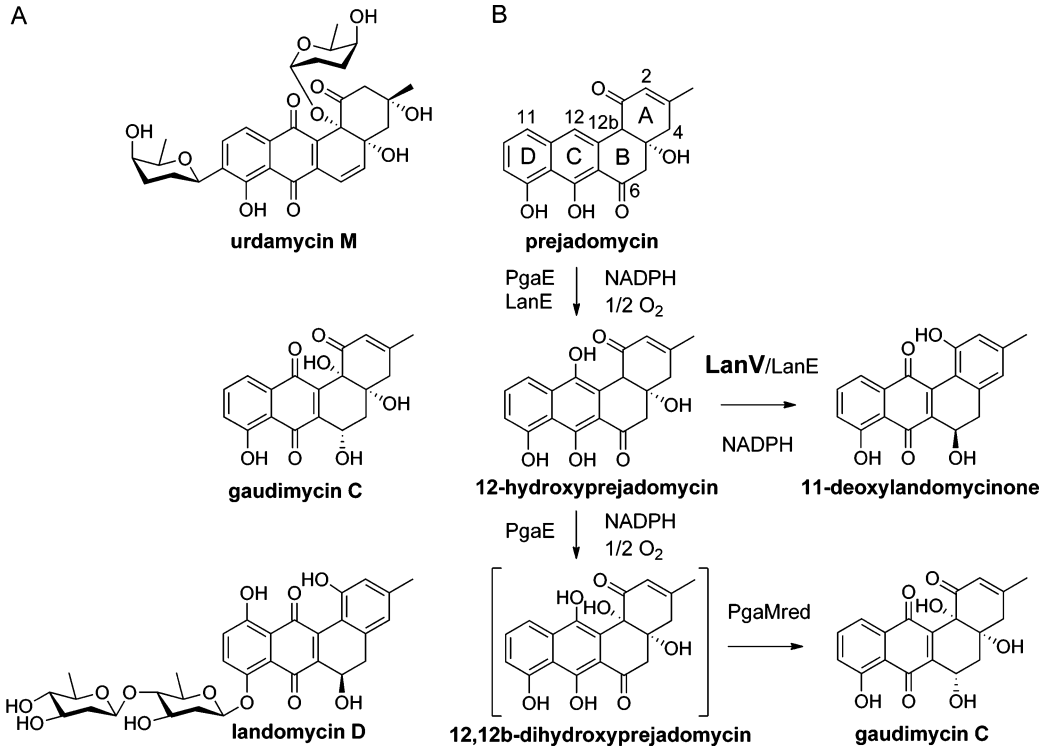

[a](A) Structures of urdamycin M, gaudimycin C, and landomycin D. (B) Tailoring reactions catalyzed by the flavoproteins LanE and PgaE, and the SDR enzymes LanV and PgaMred. The biosynthesis of urdamycins proceeds in a manner similar to that of gaudimycins, and the function of the related SDR enzyme UrdMred is identical to that of PgaMred/CabV.

redox modification regimes are responsible for the functional diversity of naturally occurring angucyclines. The key enzymes responsible for these modification steps belong to two well-characterized families, NADPH-dependent flavoprotein monooxygenases and SDRs.[17] On the gaudimycin C pathway, the flavoenzyme PgaE has been shown to utilize prejadomycin as a substrate and catalyze two consecutive hydroxylations at C-12 and C-12b, followed by ketoreduction at C-6 by the action of the SDR enzyme PgaMred (Scheme 1B).[18] The stereospecific ketoreduction by PgaMred results exclusively in the formation of the 6*S* configuration seen in gaudimycin C (Scheme 1B). On the landomycin pathway, the flavoenzyme LanE is responsible for the identical C-12 hydroxylation, but instead of an additional C-12b hydroxylation, the SDR enzyme LanV utilizes the product of the first LanE reaction for C-6 ketoreduction. Formation of 11-deoxylandomycinone with the 6*R* configuration is completed by the C-4a/C-12b dehydration catalyzed by LanE (Scheme 1B).[16,17] Interestingly, the flavoenzymes PgaE and LanE are exchangeable and able to complement the functions of each other, and the outcome of the reaction cascade is determined solely by the substrate specificity and stereoselectivity of the SDR component.[17]

Whereas the flavoprotein monooxygenases utilizing prejadomycin as a substrate have received considerable attention to date,[18−22] much less is known about the structural basis for C-6 ketoreduction, especially with regard to details of the active site architecture. Here we report the combined structural and functional analysis of LanV from *Streptomyces cyanogenus* S136. The aim of this work was to uncover the molecular basis for the control of C-6 stereochemistry in landomycin biosynthesis. For this analysis, we determined the three-dimensional crystal structures of the binary complex of LanV with $NADP^+$ and the ternary complex with $NADP^+$ and the ligand 11-deoxylandomycinone. In addition to these structural studies, the role of Tyr160 in catalysis was investigated, and the origin of the hydride transferred from NADPH to the substrate during catalysis was examined. Importantly, residue Ser192 could be identified to have an effect on the stereochemical control of the reaction.

MATERIALS AND METHODS

Expression and Purification of Recombinant Proteins. The proteins LanV,[17] PgaE,[22] and CabV[18] were overexpressed as N-terminally His-tagged fusion proteins as described previously, and the variant LanV proteins were overexpressed in the same way as native LanV. All proteins were purified to homogeneity in a single step using TALON Co^{2+} affinity resin (Clontech) in a disposable chromatography column (Bio-Rad) and eluted with 250 mM imidazole. The purity of the proteins was confirmed via sodium dodecyl sulfate−polyacrylamide gel electrophoresis, and the concentration of the proteins was estimated using the Bradford dye binding method.[23] Proteins were stored at −20 °C in 10 mM Na_3PO_4, 50 mM NaCl, 125 mM imidazole, and 50% glycerol (pH 7.6).

Crystallization, Data Collection, and Structure Determination. For crystallization, LanV was desalted using a PD-10 column (GE Healthcare) to a buffer containing 25 mM Tris, 155 mM NaCl, and 5% glycerol (pH 7.5). The enzyme was concentrated with Centriprep and Amicon Ultra devices (Millipore), and the protein concentration was determined using a NanoDrop 2000 instrument (Thermo Scientific). At an enzyme concentration of 2 mg/mL, $NADP^+$ dissolved in the

dx.doi.org/10.1021/bi400712q | *Biochemistry* 2013, 52, 5304−5314

same buffer was added to a final concentration of 1 mM, and the protein concentration was continued. The final concentrated solution was filtered with a 0.22 μm Ultrafree filter (Millipore), and $^{1}/_{10}$ volume of saturated 11-deoxylandomycinone in methanol was added. Because of interference from $NADP^+$ and 11-deoxylandomycinone, the final protein concentration of the solution could not be measured, but it was calculated to be approximately 8.1−8.6 mg/mL.

Initial crystallization experiments were performed with PACT (Molecular Dimensions) and JCSG+ screens (Qiagen). Several hits were obtained in 24 h, and the crystals were light orange in color, indicating bound ligand. The color faded within a couple of days, suggesting spontaneous degradation of the ligand over time. Crystals were optimized using the hanging drop method at room temperature. Best, saw blade-like crystals were obtained in 0.2 M sodium acetate, 0.1 M bis-tris propane (pH 6.5), and 18−20% PEG 3350. The crystals were dipped in a cryoprotectant solution [0.1 M trisodium citrate, 20% PEG 3000, and 20% PEG 400 (pH 5.5)] before they were flash-frozen in liquid nitrogen. For the LanV complex structure, saturated 11-deoxylandomycinone in methanol was added to the crystallization drops and allowed to soak into the crystals for a minimum of 10 min before the crystals were cryoprotected and frozen as described above.

Diffraction data were collected at the European Synchrotron Radiation Facility (ESRF, Grenoble, France), at beamlines ID14-4 and ID23-2. For native LanV 180° of data (720 images, 0.25° oscillation) and for LanV complex 120° of data (240 images, 0.5° oscillation) were recorded. The crystals belong to space group $P4_12_12$ with the following unit cell dimensions: $a = b = 92.50$ Å and $c = 106.30$ Å for native LanV, and $a = b = 92.61$ Å and $c = 103.33$ Å for the LanV complex. There are two protein molecules in both asymmetric units.

The data were indexed, integrated, scaled, and converted to structure factors using XDS.[24] To enhance model accuracy, high-resolution data were included regardless of the R_{sym} values as suggested by Karplus and Diederichs,[25] while maintaining acceptable values of the signal-to-noise ratio, completeness, and multiplicity of the data. For native LanV, initial phases were obtained using the automated molecular replacement pipeline BALBES[26] with the structure of *Bacillus anthracis* 3-oxoacylreductase[27] [Protein Data Bank (PDB) entry 3ICC] as a starting model (sequence identity 47.8%). An initial molecular model was built by BALBES using ARP/wARP[28] and REFMAC.[29] The LanV complex structure was determined using MOLREP[30] in the CCP4 package[31] with the native LanV structure as a search model. Both structures were refined in REFMAC interspersed with rounds of manual model building in Coot.[32] The PRODRG server[33] was used to create the necessary coordinate files for the ligand. Water molecules were added to the structures in Coot and inspected manually, keeping only those with electron density above 1σ and *B* values of <55. The structures were validated using the MolProbity server.[34] The Ramachandran outliers in Table 1 are Ser146 (in both chains in both structures) forming part of the NADP binding site and Thr208 (ternary complex structure) located in a region of poor electron density in helix α7 adjacent to the bound substrate. Details of the data collection and refinement statistics are listed in Table 1. Figures depicting protein structures were prepared using PyMol (The PyMOL Molecular Graphics System, version 1.3, Schrödinger, LLC) unless otherwise stated.

Mutagenesis of *lanV*. The mutagenesis of *lanV* was conducted using a modified four-primer overhang extension polymerase chain reaction (PCR) method.[21,35] The *lanV* gene was first amplified from template pBHBΔ/LanV[17] as N- and C-terminal fragments, containing overlapping modified complementary ends, generated by the mutagenesis primers used in combination with the outer primers (Table S1 of the Supporting Information). The primary amplification products were then mixed together and used as a template for the PCR with the outer primers to produce the final full-length mutated *lanV*. The product was then extracted and subcloned into pBHBΔ[36] as a *Bgl*II−*Hind*III fragment and confirmed by sequencing (Eurofins MWG Operon).

Enzyme Reactions *in Vitro*. *In vitro* enzyme reactions were conducted under conditions described previously.[20] The enzyme concentrations used in the reactions were as follows: 75−150 nM PgaE, 300 nM LanV, 1.2 μM LanV Tyr160Ala, 400 nM LanV Ser192Ile, and 600 nM CabV. Isolation of substrate and products from *in vitro* reactions was performed with repeated chloroform extractions as described previously.[20] The deuterium-labeled $NADP^2H$ was prepared *in vitro* using glucose dehydrogenase from *Bacillus megaterium*.[37] The reaction mixture containing 10 mM [1-^{2}H]-D-glucose, 80 μM $NADP^+$, and 1.6 units of glucose dehydrogenase was incubated at 23 °C for 1 h; the enzymes were removed with chloroform precipitation, and the prepared $NADP^2H$ solution was used to produce 11-deoxylandomycinone from 40 μM prejadomycin by PgaE and LanV.

High-Performance Liquid Chromatography (HPLC) Analysis of the Substrate and Products. The compounds extracted from reactions were analyzed by reverse-phase HPLC (RP-HPLC) (Shimadzu VP series chromatography system with a diode array detector, SPD-M10Avp, Merck LiChrospher 100 RP-18/5 μm column, gradient from 15% acetonitrile with 0.1% HCOOH to 100% acetonitrile, at a flow rate of 0.5 mL/min with a T_{tot} of 60 min). The substrate prejadomycin and the products 11-deoxylandomycinone and gaudimycin C were identified on the basis of retention times and UV−vis spectra and compared on the basis of the peak areas at 256 nm.

Liquid Chromatography−Mass Spectrometry (LC−MS) Analysis. MS analysis of the deuterium-labeled 11-deoxylandomycinone was performed with a Micromass Quattro Premier tandem quadropole mass spectrometer (Waters Corp.) using positive ESI connected to an RP-HPLC system (Waters Acquity UPLC system, Waters SunFire C18/3.5 μm column, gradient from 15% acetonitrile with 0.1% HCOOH to 100% acetonitrile, at a flow rate of 0.25 mL/min with a T_{tot} of 45 min). The capillary voltage was set to 3 kV and the sample cone voltage to 30 V. The source and the desolvation temperatures were set to 130 and 150 °C, respectively. Nitrogen was used as the desolvation (400 L/h) and cone (50 L/h) gas.

Gel Filtration Analysis. Gel filtration analysis was performed with a Shimadzu VP series HPLC system with a diode array detector [SPD-M10Avp, Tosoh Biosciences TSKgel SuperSW2000/4.0 μm column, isocratic run with 100 mM potassium phosphate buffer (pH 7.6), at a flow rate of 0.16 mL/min with a T_{tot} of 30 min]. The analyzed samples consisted of 60 μg of LanV, 60 μg of PgaE, and 50 μg of bovine serum albumin; all samples were in 100 mM potassium phosphate buffer (pH 7.6).

RESULTS AND DISCUSSION

Structure Determination of LanV and Quality of the Electron Density Maps. LanV (27.3 kDa) was crystallized in the presence of $NADP^+$ and the reaction product 11-deoxylandomycinone. The structure was determined by molecular replacement using a putative 3-oxoacyl-(acyl carrier protein) reductase from *B. anthracis*[27] (PDB entry 3ICC) as a search model and refined to 1.65 Å resolution. Electron density could be traced for the whole polypeptide chain, although the density was poor in one loop region comprising residues Ala198−Arg206 in one of the two protein molecules found in the asymmetric unit. On the basis of electron density, one molecule of $NADP^+$ could be found bound to each polypeptide chain, but 11-deoxylandomycinone had apparently degraded during crystallization, because instead of the ligand only one molecule of acetic acid from the crystallization conditions was present in the active site. To obtain the structure of LanV in complex with a ligand, additional 11-deoxylandomycinone was soaked into the crystals and the resulting diffraction data were refined to 2.0 Å resolution. The quality of the electron density maps (Figure S1 of the Supporting Information) and refinement statistics (Table 1) were in good agreement with the obtained resolutions.

Overall and Quaternary Structure of LanV. The overall structure of LanV is that of a Rossmann fold, as expected for an enzyme of the SDR family (Figure 1A). The protein structure is dominated by a central seven-stranded parallel β-sheet, which is surrounded by six parallel α-helices, three on each side. This classical supersecondary structure provides a platform for dinucleotide binding,[38] and the characteristic N-terminal TGXXXGXG motif (pink, Figure 2), which forms a tight loop that provides sufficient space for binding of the dinucleotide,[38] is present in LanV. The active site cleft is formed between two ridges consisting of loop and α-helical segments residing on top of the core structure (Figure 1A). The larger of these crests is formed by two loop regions that reside between the $\beta4-\alpha4$ and $\beta5-\alpha6$ secondary structure elements, while the smaller flaplike structure is composed of the short $\alpha7$ helix and the surrounding loop areas (Figure 2).

Both the crystal structure (Figure 1B) and its PISA analysis[39] (Table S2 of the Supporting Information) suggest that LanV is a tetramer like many other SDR enzymes. However, on the basis of gel filtration experiments (Figure S2 of the Supporting Information), the enzyme appears to be a dimer in solution. It has been shown previously that SDR enzymes may exist in different oligomeric states and that the equilibrium between the states is in some cases affected by ligands and cosubstrates,[40,41] which were not present under our experimental conditions. Therefore, it seems likely that LanV, like clavulanic acid dehydrogenase,[40] exists in both dimeric and tetrameric forms depending on the conditions. The two dimerization interfaces, which appear to be mostly conserved between LanV and the related angucycline 6-ketoreductases (Figure 2), are similar in nature and consist of both ionic and hydrophobic interactions (Table S2 of the Supporting Information). The first interface is formed through stacking of α-helices $\alpha4-\alpha6$ of both subunits (Table S2 of the Supporting Information, monomers A+A′ and B+B′), whereas the second involves interactions mainly between elements $\alpha8$ and $\beta7$ of both subunits (Table S2 of the Supporting Information, monomers A+B). Because the calculated strengths of both interfaces appear to be similar based on the PISA analysis, it is difficult to assess which one of the dimers was observed in the gel filtration experiment. However, it may be possible that the dimerization interface between monomers A+A′ and B+B′ was disrupted under the experimental conditions, because helices $\alpha5$ and $\alpha6$ are also in contact with the cosubstrate NADPH.

Table 1. X-ray Data Collection and Crystallographic Refinement Statistics[a]

	LanV (empty)	LanV (LANDO)
	Data Collection	
PDB entry	4KWH	4KWI
X-ray source	ESRF ID14-4	ESRF ID23-2
space group	$P4_12_12$	$P4_12_12$
unit cell (Å)	$a = b = 92.50$, $c = 106.30$	$a = b = 92.61$, $c = 103.33$
resolution (Å)	46.0−1.65 (1.69−1.65)	50−2.0 (2.05−2.00)
wavelength (Å)	0.9393	0.8726
no. of unique reflections	56150	31692
multiplicity	14.1 (13.9)	7.2 (6.9)
completeness (%)	99.7 (68.6)	99.1 (90.9)
mean $\langle I\rangle/\langle\sigma_I\rangle$	27.2 (4.1)	12.1 (2.1)
R_{sym} (%)[b]	6.6 (68.8)	13.7 (92.9)
Wilson B factor (Å^2)	26.0	31.9
	Refinement	
R factor (all reflections) (%)	14.9	18.4
R_{free} (%)[c]	17.6	22.5
no. of atoms	3814	3713
no. of water molecules	445	239
no. of other molecules[d]	2 NADP, 2 ACY, 2 PEG	2 NADP, PEG, 2 LANDO
rmsd for bond lengths (Å)	0.010	0.009
rmsd for bond angles (deg)	1.345	1.366
average B factor (Å^2)		
all atoms	20.8	27.0
protein	19.8	26.8
waters/other molecules[d]	30.1/NADP 15.8/ACY 23.8/PEG 43.2	30.1/NADP 22.7/PEG 47.7/LANDO 37.1
Ramachandran plot (%)		
favored regions	444 (96.7)	474 (95.4)
allowed regions	13 (2.8)	20 (4.0)
outliers	2 (0.4)	3 (0.6)

[a]Values in parentheses are for the highest-resolution shell. [b]$R_{sym} = [\sum_h\sum_i|I_i(h) - \langle I(h)\rangle|]/[\sum_h\sum_I I(h)]$, where $I_i(h)$ is the ith measurement of reflection h and $\langle I(h)\rangle$ is the weighted mean of all measurements of h. [c]Five percent of the reflections were used in the R_{free} calculations. [d]NADP, nicotinamide adenine dinucleotide phosphate; ACY, acetate; PEG, polyethylene glycol; LANDO, 11-deoxy-6-oxylandomycinone.

Comparison of the Structure of LanV to Related Proteins. A comparison to known protein structures using the Dali server[42] shows LanV to be most similar in overall fold to fatty acid ketoreductases such as *B. anthracis* short-chain dehydrogenase/reductase[27] with a Z score of 40, a root-mean-square deviation of 1.2 Å, and a sequence identity of 47%. The level of similarity of LanV to homologous enzymes involved in natural product biosynthesis is somewhat lower, with Z scores of 32, 32, and 30, rmsd's of 1.7, 1.7, and 2.4 Å, and levels of sequence identity of 28, 24.5, and 25% for *Streptomyces*

dx.doi.org/10.1021/bi400712q | *Biochemistry* 2013, 52, 5304−5314

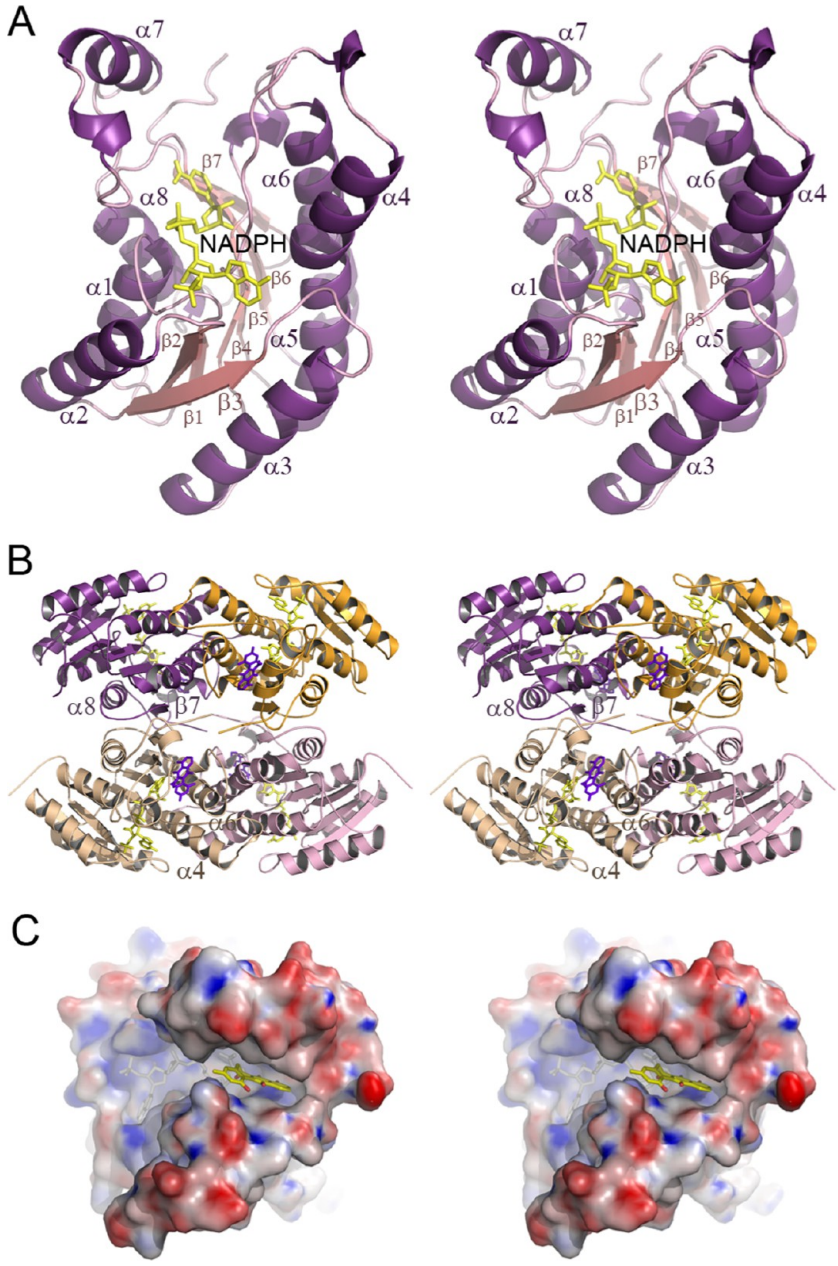

Figure 1. Stereoview images of the overall structure of the landomycin 6-ketoreductase LanV. (A) The Rossmann fold of the LanV monomer provides a binding site for $NADP^+$ on top of the β-sheet secondary structure. (B) Structure of the LanV tetramer. (C) Surface view of LanV with calculated electrostatics demonstrating the hydrophobic binding site of the ligand. The surface is colored according to the electrostatic potential at 23 °C (−22 to 22 kT/e) with positive potential colored blue and negative potential colored red.

coelicolor actinorhodin polyketide ketoreductase ActKR,[43,44] *Streptomyces griseoruber* hedamycin type II polyketide ketoreductase HedKR,[14] and *Streptomyces clavuligerus* clavulanic acid dehydrogenase,[40] respectively.

The largest structural differences between LanV and related ketoreductases involved in natural product biosynthesis can be found in the α7 flaplike structure (LanV residues 195−217), which is positioned in a manner that leaves the active site accessible to bulk solvent. This is in stark contrast to ActKR and HedKR, where the corresponding region prior to helix α7 is 11 residues longer (green, Figure 2) and which forms an additional helix over the active site that is not present in LanV. Consequently, the helix−turn−helix motif has been suggested to adopt both open and closed conformations during the catalytic cycle.[14,15,43] In clavulanic acid dehydrogenase, the lid region extends even farther over the cleft closing the active site into a narrow tunnel.[40] Similar movement for the lid helix has been observed in the more distantly related catalytic domains of EryKR1,[45] TylKR1,[46] and AmpKR2[47] ketoreductases involved in the biosynthesis of type I polyketides erythromycin, tylosin, and amphotericin, respectively. The second major structural difference can be found in the loop regions before and after α3 (residues 66−69 and 85−90) at the far edge of the NADPH binding site. The loop region after α3 is six residues longer in LanV (green, Figure 2), which results in a subtle tilt of helix α3 in comparison to the structures of ActKR and HedKR. Overall, the two areas of LanV discussed above resemble more closely fatty acid ketoreductases both in length and in the

dx.doi.org/10.1021/bi400712q | *Biochemistry* 2013, 52, 5304−5314

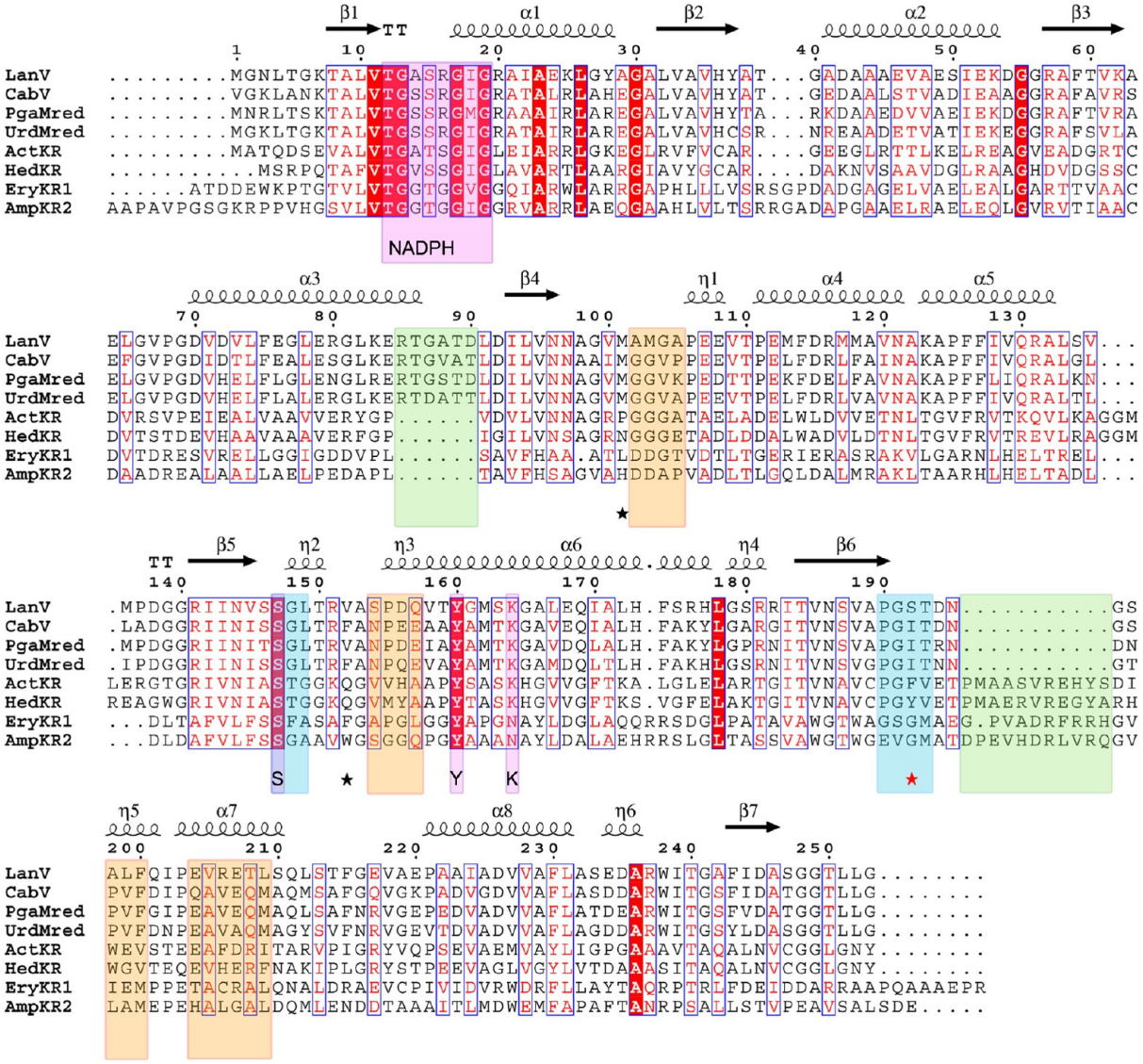

Figure 2. Structure-based multiple-sequence alignment of LanV, the related angucycline 6-ketoreductases CabV, PgaMred, and UrdMred, the type II ketoreductases ActKR and HedKR, and the modular type I ketoreductases EryKR1 and AmpKR2. Only the catalytic domains of EryKR1 and AmpKR2 are included in the alignment.[45,47] The sequence motifs for $NADP^+$ binding and catalysis are highlighted in pink. The regions in contact with rings C and D of the ligand are highlighted in turquoise. Regions near rings A and B are highlighted in orange. The extended loop region after α3 in C6-ketoreductases and the lid region of type I and type II ketoreductases are highlighted in green. Residues discussed in the context of the stereoselectivity of the reaction are denoted with stars.

conformation of the elements than the related enzymes from *Streptomyces*.

Binding of the Cosubstrate $NADP^+$. The $NADP^+$ molecule is bound in an extended conformation on top of the central β-sheet that positions the nicotinamide ring of the cosubstrate toward the active site cleft (Figure 3A). LanV has been shown to be able to utilize both NADH[16] and NADPH[17] for catalysis, but the tridentate coordination of the backbone amide groups of residues Ala38−Gly40 to the 2′-phosphate group of the cosubstrate would suggest a preference for the latter. In addition, the conserved residue Arg16 (Figure 2) found within hydrogen bonding distance of the phosphate group is likely to be involved in the selection of the cosubstrate (Figure 3B), as has been suggested for other members of the SDR family.[38]

Binding of the Ligand 11-Deoxylandomycinone. The active site is lined with mostly hydrophobic amino acids that are situated in the surrounding α-helical segments on both sides of the cavity (Figure 1C). Consistent with this, the structure of LanV in complex with the landomycinone ligand at 2.0 Å resolution demonstrates that residues Met101, Met103, Leu149, Val152, Leu199, Phe200, Val205, Leu209, Leu212, and possibly Thr250 form a deep crevice complementary to the shape of the relatively planar polyaromatic ligand (Figure 3C), which positions the substrate for catalysis mainly through hydrophobic interactions. The chief electrostatic interactions with the ligand are derived solely from Gln157, Ser192, and the nicotinamide ring of $NADP^+$ that resides at the bottom of the active site. The binding of the substrate does not appear to induce large conformational changes in LanV, and it would seem that the active site remains in an open configuration during catalysis. This significant difference from related SDR enzymes[14,15,43,45−48] may be due to the truncated α7 flap region, which is too short to form a lid over the active site. The

dx.doi.org/10.1021/bi400712q | *Biochemistry* 2013, 52, 5304−5314

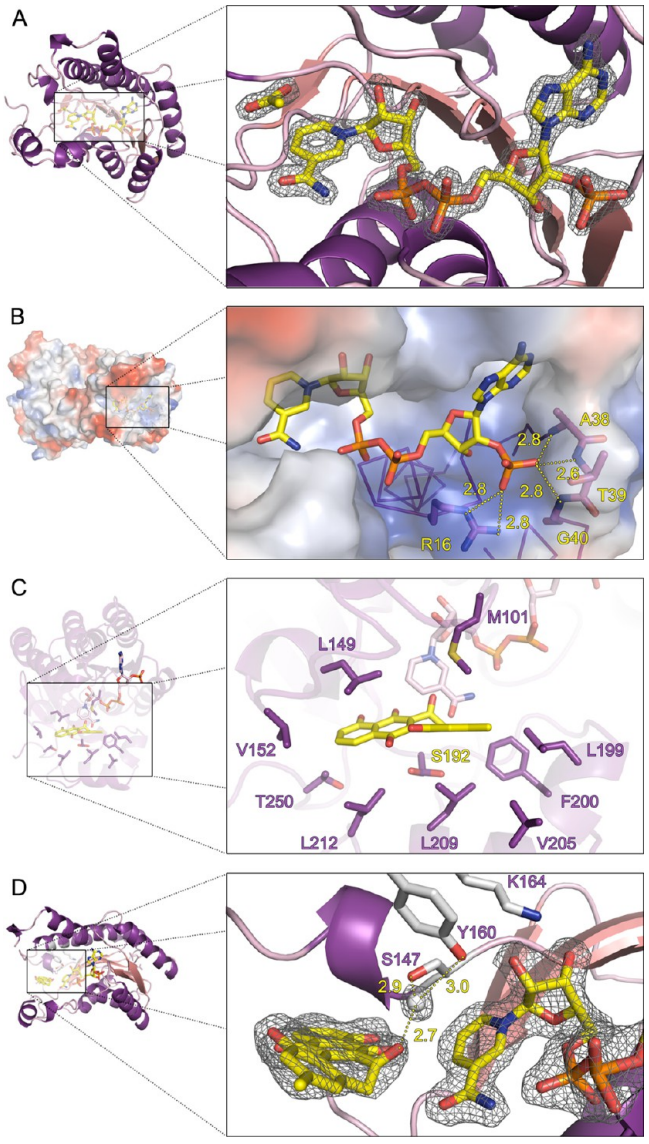

Figure 3. Molecular architectures of ligand and cosubstrate binding sites of LanV. (A) Binding of $NADP^+$ and acetic acid to LanV at 1.65 Å resolution (σ = 1.0). (B) Hydrogen bonding network to the 2′-phosphate group of the adenine unit of $NADP^+$ depicted in angstroms. (C) Amino acid residues responsible for shaping the hydrophobic active site of LanV. The residue Ser192 could be observed in two alternative conformations. (D) View of the active site of LanV with the catalytic residues Ser147, Tyr160, and Lys164 highlighted and the hydrogen bonding distance to the catalytic water molecule shown. The electron density of 11-deoxylandomycinone (σ = 1.0) could be best fit with a 6-keto form of the compound. The ligands and cosubstrates were omitted from calculation of the electron density maps ($2F_o - F_c$) to reduce model bias.

overall structures of the binary and ternary complexes are very similar with an rmsd of 0.2 Å (Z score of 46.6). The most obvious alteration in the active site can be seen in Met101, which has two different conformations in the two structures. In the unliganded structure, Met101 is bent toward $NADP^+$, whereas in the ternary complex, the residue is tilted toward Gln157 and the C-6 group of the ligand.

Mechanism of 6-Ketoreduction. Detailed inspection of the electron density map of the ternary complex revealed that the density fit best the 6-keto form of 11-deoxylandomycinone, suggesting that the reaction had proceeded in the reverse direction in the crystals. The ligand is positioned above the nicotinamide ring of the cosubstrate, and the conserved residues Ser147, Tyr160, and Lys164 (pink, Figure 2) are found nearby well positioned for catalysis (Figure 3D). Consequently, the Tyr160Ala mutation resulted in the complete loss of enzymatic activity of LanV (Figure 4A,B).

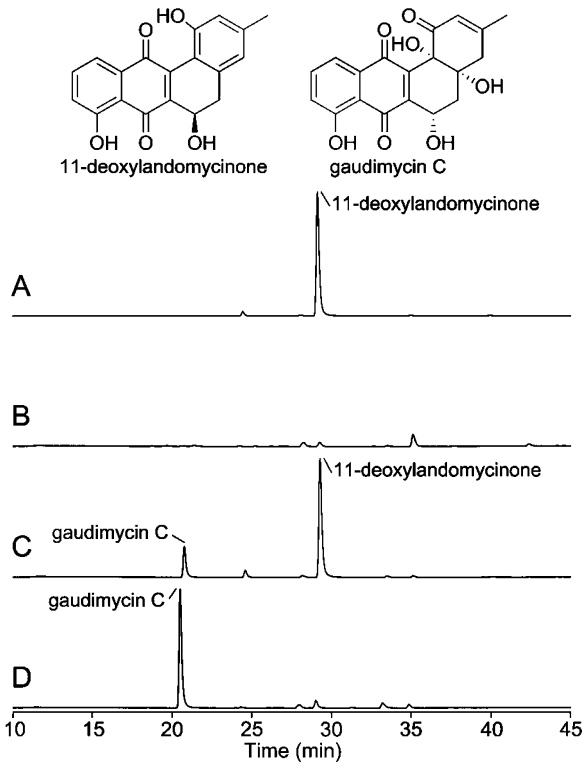

Figure 4. HPLC chromatograms of *in vitro* reactions conducted with prejadomycin as a substrate monitored at 428 nm and structures of the reaction products 11-deoxylandomycinone and gaudimycin C with 6*R* and 6*S* stereochemistry, respectively. (A) Control reaction with PgaE and LanV producing 11-deoxylandomycinone. (B) Reaction with PgaE and the LanV Tyr160Ala variant that does not lead to formation of 11-deoxylandomycinone. In the absence of a functional 6-ketoreductase, the reaction product of PgaE degrades in solution.[17,18] (C) Reaction with PgaE and LanV Ser192Ile producing both gaudimycin C and 11-deoxylandomycinone in a 1:3 ratio. (D) Control reaction with PgaE and CabV producing gaudimycin C.

The role of these residues has been extensively studied in classical SDR enzymes,[49,50] and they have been proposed to be responsible for protonation of the carbonyl group of the substrate. The tyrosine residue has been identified as a general acid, while the lysine lowers the pK_a value of the tyrosine, thus aiding proton transfer. The conserved serine has been suggested to be important for stabilization of the substrate.[50] LanV lacks the fourth conserved asparagine residue, which forms the final amino acid of the canonical catalytic tetrad of SDR enzymes.[49] Somewhat unexpectedly, a coordinated water molecule lies between the ligand and the catalytic Tyr160, indicating that it may be used to mediate proton transfer (Figure 3D). The water molecule also coordinates to Ser147, which resides 5.0 Å from the C-6 group of the ligand, indicating that the residue may not be required for polarization of the carbonyl group of the substrate in LanV. This unusual arrangement may be requisite because of the deep and narrow shape of the active site cleft (Figure 1C), which may prevent

dx.doi.org/10.1021/bi400712q | *Biochemistry* 2013, 52, 5304−5314

protrusion of the substrate within direct hydrogen bonding distance of Ser147 and Tyr160.

In addition to protonation by Tyr160, the reaction mechanism of SDR ketoreductases involves transfer of a hydride from NADPH to the substrate.[51] To demonstrate that the hydride originates from the 4-*pro-S* side of the cosubstrate, stereospecifically labeled deuterated NADP^{2}H was generated enzymatically and utilized in LanV reactions as described in Materials and Methods. Analysis of the reaction product 11-deoxylandomycinone by LC−MS revealed that the mass had increased by 0.99 Da, which is consistent with the incorporation of one deuterium atom (Figure 5).

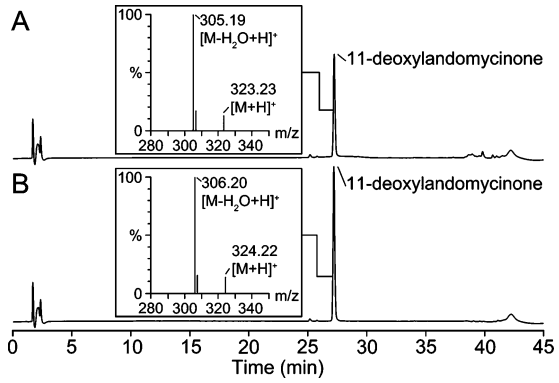

Figure 5. Demonstration of incorporation of deuterium from the 4-*pro-S* face of NADPH in a coupled reaction with PgaE and LanV by LC−ESI-MS. (A) Control reaction. (B) A reaction conducted using labeled NADP^{2}H leads to an increase in the mass of the [M + H] molecular ion of 0.99 Da.

In conclusion, the structural and functional analysis of LanV promotes a catalytic model in which the reaction is initiated by the transfer of a proton from Tyr160 to the C-6 carbonyl group of the substrate, possibly via the catalytic water molecule, and followed by transfer of the 4-*pro-S* hydride from the cosubstrate NADPH to C-6 of the substrate (Figure 6).

Relationship to Related Angucycline 6-Ketoreductases and Other SDR Enzymes Involved in Antibiotic Biosynthesis. We have previously speculated that landomycins are the more recently evolved angucyclines due to the observation that the flavoprotein LanE is capable of catalyzing C-12b hydroxylation even though there is no

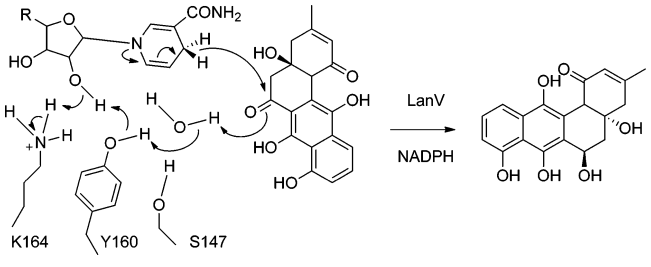

Figure 6. Proposed reaction mechanism of LanV. The catalysis of the 6-ketoreduction starts with the transfer of a proton from Tyr160 via a coordinated water molecule to the 6-carbonyl of the substrate, and the 4-*pro-S* hydride of the NADPH is transferred to C-6 of the substrate. The proton relay system is likely to involve the 2′-hydroxyl group of the ribose unit of NADPH and the ε-amino group of Lys164, in addition to the hydroxyl group of Tyr160 and the coordinated water molecule. R is adenoside-2′-phosphate-5′-diphosphate.

requirement for the activity in landomycin biosynthesis.[17] The distinguishing feature in the evolution of landomycins has therefore been a shift in the substrate specificity and stereoselectivity of LanV in comparison to those of the homologous UrdMred and CabV/PgaMred involved in the biosynthesis of urdamycins and gaudimycin, respectively (Scheme 1). In the absence of a crystal structure of an enzyme catalyzing 6-ketoreduction with the *R* configuration, it is challenging to pinpoint the exact evolutionary events that have led to the conversion of enzymatic activity, but some clues may be acquired from the structure-based multiple-sequence alignment (Figure 2) and experiments conducted with related SDR enzymes involved in antibiotic biosynthesis.

An early step in the biosynthesis of many aromatic type II polyketides, including angucyclines, includes ketoreduction of a specific carbonyl group of the ACP-bound polyketide chain.[6,12] Functional studies of the SDR enzymes ActKR[52] and HedKR[14] involved in actinorhodin and hedamycin biosynthesis, respectively, have uncovered "PGG" and "NGG" motifs that have an effect on the stereoselectivity of the promiscuous activity of the enzymes, the oxidation of the unnatural substrate tetralol. In the case of ActKR, a Pro94Leu single-point mutation has been shown to be sufficient for altering the stereoselectivity of the reaction,[52] while experiments with HedKR suggested that additional changes in the enzyme are required for the conversion of activity.[14] In modular type I PKSs, SDR domains are responsible for determination of the stereochemistry of the β-hydroxyl groups of nascent polyketide chains. The "LDD" sequence motif, which corresponds to the "PGG" and "NGG" motifs of aromatic polyketide ketoreductases, and "W" sequence motif have been hypothesized to guide the ACP-tethered polyketides into the active site in alternate substrate orientations, which in turn determines the stereochemical outcome of ketoreduction.[53] Mutagenesis studies with EryKR1[45] and AmpKR2[47] domains from the erythromycin and amphotericin pathways have indeed confirmed that these motifs influence enzymatic activity, but they do not appear to be solely responsible for the stereochemical control of the reaction. However, the structure-based multiple-sequence alignment (Figure 2) suggests that these sequence motifs may not be the key amino acids affecting stereoselectivity in angucycline 6-ketoreduction, because Pro94 of ActKR (PGG motif) and Trp359 of AmpKR2 (W motif) correspond to the conserved Met101 and the semiconserved Val152 in LanV, respectively. Therefore, we decided to focus instead on residue Ser192, which resides on the opposite side of the ligand from Met101 and Val152 (Figure 3C), as the equivalent amino acid in enzymes catalyzing 6*S* stereochemisty is a bulkier isoleucine (Figure 2).

Engineering the Activity of LanV and Further Stereochemical Considerations. Consistent with the analysis described above, the single mutant LanV Ser192Ile was able to convert prejadomycin to both gaudimycin C and 11-deoxylandomycinone in a 1:3 ratio on the basis of integration of HPLC peak areas at 256 nm (Figure 4C,D) in a coupled reaction with PgaE. This result demonstrated that the single-amino acid substitution switched, in part, both the substrate specificity (12-hydroxyprejadomycin vs 12,12b-dihydroxyprejadomycin) and stereoselectivity (6*R* vs 6*S*) of the enzyme (Scheme 1B). While the exact mechanism through which Ser192, which is quite distal from the 6-keto group, affects the stereochemistry remains elusive, it may be that the role of Ser/Ile192 is to participate in determining the correct positioning

dx.doi.org/10.1021/bi400712q | *Biochemistry* 2013, 52, 5304−5314

and tilt of the rigid and fairly planar substrate to enforce the desired stereochemical outcome. It is unlikely that the two conformations observed for Ser192 in the LanV ternary complex (Figure 3C) have any critical role in catalysis, other than to indicate a lack of tight coordination to the substrate.

Nonetheless, it is evident that a single-amino acid change is not sufficient for complete restoration of the ancestral enzymatic activity of LanV. There appear to be surprisingly many changes in the amino acids responsible for the formation of the two large hydrophobic walls in the active site cleft, especially if the high level of sequence identity of LanV with the functionally distinct angucycline 6-ketoreductases (approximately 68%) is considered. Whereas the loop regions after β5 and β6, which form the back end of the active site and are in contact with rings C and D of the substrate, are well-conserved apart from the aforementioned Ser192 (turquoise, Figure 2), the majority of amino acids found near rings A and B are highly dissimilar (orange, Figure 2). In particular, the sequence of α7 that forms the majority of one of the sides of the active site has gone through various mutations in angucycline ketoreductases. It is particularly interesting to note that unlike in LanV, in many related enzymes the larger structurally equivalent α6–α7 lid region is mobile[48] and has been suggested to be involved in substrate selection upon closure of the active site cleft.[15,47] Taken together, it may be that the major contributor to the alignment of the substrates for either 6*R* or 6*S* ketoreduction may be the overall shape of the hydrophobic active site crevice, which in turn may be determined by long-range effects and the combined influence of the 20-odd residues that line the cavity. Experiments that aim at a comprehensive understanding of the apparently complex structure–function relationships of the angucycline 6-ketoreductases are currently in progress in our laboratory.

CONCLUDING REMARKS

Natural products isolated from Actinomycetes have remained at the forefront of drug discovery ever since the discovery of streptomycin in 1944.[54] Over the years, natural products have intrigued chemists who have been fascinated by the complex chemical structures of these molecules and the multitude of chiral carbons present. Structural studies of enzymes involved in the biosynthesis of these metabolites have recently begun to shed light on how the producing organisms are able to catalyze asymmetric synthesis with such efficiency. In aromatic polyketide biosynthesis, it has become apparent that hydrophobic interactions are especially important for the correct alignment of the substrate in the active site and that specificity appears to be controlled mainly by the shape of the binding pocket rather than through specific hydrogen bonds. Examples of enzymes other than LanV with such large hydrophobic cavities are the flavoprotein monooxygenases PgaE[22] and RdmE[55] from the gaudimycin and rhodomycin pathways and the quinone-forming cofactor independent oxygenases ActVA-6[56] and SnoaB[57] involved in actinorhodin and nogalamycin biosynthesis. This paradigm of substrate recognition may be a considerable challenge for structure-based protein engineering of antibiotic biosynthesis enzymes, because the enzymatic activity may be determined by the cumulative effects of minor differences in multiple regions, as has recently been shown for PgaE.[21]

ASSOCIATED CONTENT

Supporting Information

Electron density maps of the LanV structures, results of the gel filtration analysis, results of the PISA analysis, and oligonucleotide primers used in this study. This material is available free of charge via the Internet at http://pubs.acs.org.

Accession Codes

Coordinates and structure factors have been deposited in the Protein Data Bank as entries 4KWH and 4KWI.

AUTHOR INFORMATION

Corresponding Author

*E-mail: mikko.mk@gmail.com. Telephone: +35823336847. Fax: +35823336860.

Author Contributions

P. Paananen and P. Patrikainen contributed equally to this work.

Funding

This study was supported by the Academy of Finland (127844 to P.M. and 136060 to M.M.-K.) and the National Graduate School in Informational and Structural Biology.

Notes

The authors declare no competing financial interest.

ACKNOWLEDGMENTS

We gratefully acknowledge access to synchrotron radiation at the European Synchrotron Radiation Facility and the help of Dr. Jukka-Pekka Suomela with the MS analysis.

ABBREVIATIONS

ACP, acyl carrier protein; PKS, polyketide synthase; rmsd, root-mean-square deviation; SDR, short-chain alcohol dehydrogenase/reductase.

REFERENCES

(1) Newman, D. J., and Cragg, G. M. (2012) Natural products as sources of new drugs over the 30 years from 1981 to 2010. *J. Nat. Prod.* 75, 311–335.

(2) Bahrami, F., Morris, D. L., and Pourgholami, M. H. (2012) Tetracyclines: Drugs with huge therapeutic potential. *Mini Rev. Med. Chem.* 12, 44–52.

(3) Weiss, R. B. (1992) The anthracyclines: Will we ever find a better doxorubicin? *Semin. Oncol.* 19, 670–686.

(4) Antal, N., Fiedler, H. P., Stackebrandt, E., Beil, W., Stroch, K., and Zeeck, A. (2005) Retymicin, galtamycin B, saquayamycin Z and ribofuranosyllumichrome, novel secondary metabolites from *Micromonospora sp.* Tu 6368. I. Taxonomy, fermentation, isolation and biological activities. *J. Antibiot.* 58, 95–102.

(5) Jakeman, D. L., Bandi, S., Graham, C. L., Reid, T. R., Wentzell, J. R., and Douglas, S. E. (2009) Antimicrobial activities of jadomycin B and structurally related analogues. *Antimicrob. Agents Chemother.* 53, 1245–1247.

(6) Kharel, M. K., Pahari, P., Shepherd, M. D., Tibrewal, N., Nybo, S. E., Shaaban, K. A., and Rohr, J. (2012) Angucyclines: Biosynthesis, mode-of-action, new natural products, and synthesis. *Nat. Prod. Rep.* 29, 264–325.

(7) Weber, S., Zolke, C., Rohr, J., and Beale, J. M. (1994) Investigations of the biosynthesis and structural revision of landomycin A. *J. Org. Chem.* 59, 4211–4214.

(8) Rohr, J., and Zeeck, A. (1987) Metabolic products of microorganisms. 240. Urdamycins, new angucycline antibiotics from *Streptomyces fradiae*. II. Structural studies of urdamycins B to F. *J. Antibiot.* 40, 459–467.

(9) Palmu, K., Ishida, K., Mäntsälä, P., Hertweck, C., and Metsä-Ketelä, M. (2007) Artificial reconstruction of two cryptic angucycline antibiotic biosynthetic pathways. *ChemBioChem 8*, 1577−1584.
(10) Ostash, B., Korynevska, A., Stoika, R., and Fedorenko, V. (2009) Chemistry and biology of landomycins, an expanding family of polyketide natural products. *Mini Rev. Med. Chem. 9*, 1040−1051.
(11) Korynevska, A., Heffeter, P., Matselyukh, B., Elbling, L., Micksche, M., Stoika, R., and Berger, W. (2007) Mechanisms underlying the anticancer activities of the angucycline landomycin E. *Biochem. Pharmacol. 74*, 1713−1726.
(12) Hertweck, C., Luzhetskyy, A., Rebets, Y., and Bechthold, A. (2007) Type II polyketide synthases: Gaining a deeper insight into enzymatic teamwork. *Nat. Prod. Rep. 24*, 162−190.
(13) Metsä-Ketelä, M., Palmu, K., Kunnari, T., Ylihonko, K., and Mäntsälä, P. (2003) Engineering anthracycline biosynthesis toward angucyclines. *Antimicrob. Agents Chemother. 47*, 1291−1296.
(14) Javidpour, P., Das, A., Khosla, C., and Tsai, S. C. (2011) Structural and biochemical studies of the hedamycin type II polyketide ketoreductase (HedKR): Molecular basis of stereo- and regiospecificities. *Biochemistry 50*, 7426−7439.
(15) Korman, T. P., Tan, Y. H., Wong, J., Luo, R., and Tsai, S. C. (2008) Inhibition kinetics and emodin cocrystal structure of a type II polyketide ketoreductase. *Biochemistry 47*, 1837−1847.
(16) Kharel, M. K., Pahari, P., Shaaban, K. A., Wang, G., Morris, C., and Rohr, J. (2012) Elucidation of post-PKS tailoring steps involved in landomycin biosynthesis. *Org. Biomol. Chem. 10*, 4256−4265.
(17) Patrikainen, P., Kallio, P., Fan, K., Klika, K. D., Shaaban, K. A., Mäntsälä, P., Rohr, J., Yang, K., Niemi, J., and Metsä-Ketelä, M. (2012) Tailoring enzymes involved in the biosynthesis of angucyclines contain latent context-dependent catalytic activities. *Chem. Biol. 19*, 647−655.
(18) Kallio, P., Patrikainen, P., Suomela, J. P., Mäntsälä, P., Metsä-Ketelä, M., and Niemi, J. (2011) Flavoprotein hydroxylase PgaE catalyzes two consecutive oxygen-dependent tailoring reactions in angucycline biosynthesis. *Biochemistry 50*, 5535−5543.
(19) Chen, Y., Fan, K., He, Y., Xu, X., Peng, Y., Yu, T., Jia, C., and Yang, K. (2010) Characterization of JadH as an FAD- and NAD(P)H-dependent bifunctional hydroxylase/dehydrase in jadomycin biosynthesis. *ChemBioChem 11*, 1055−1060.
(20) Kallio, P., Liu, Z., Mäntsälä, P., Niemi, J., and Metsä-Ketelä, M. (2008) Sequential action of two flavoenzymes, PgaE and PgaM, in angucycline biosynthesis: Chemoenzymatic synthesis of gaudimycin C. *Chem. Biol. 15*, 157−166.
(21) Kallio, P., Patrikainen, P., Belogurov, G. A., Mäntsälä, P., Yang, K., Niemi, J., and Metsä-Ketelä, M. (2013) Tracing the evolution of angucyclinone monooxygenases: Structural determinants for C-12b hydroxylation and substrate inhibition in PgaE. *Biochemistry 52*, 4507−4516.
(22) Koskiniemi, H., Metsä-Ketelä, M., Dobritzsch, D., Kallio, P., Korhonen, H., Mäntsälä, P., Schneider, G., and Niemi, J. (2007) Crystal structures of two aromatic hydroxylases involved in the early tailoring steps of angucycline biosynthesis. *J. Mol. Biol. 372*, 633−648.
(23) Bradford, M. M. (1976) A rapid and sensitive method for the quantitation of microgram quantities of protein utilizing the principle of protein-dye binding. *Anal. Biochem. 72*, 248−254.
(24) Kabsch, W. (2010) Integration, scaling, space-group assignment and post-refinement. *Acta Crystallogr. D66*, 133−144.
(25) Karplus, P. A., and Diederichs, K. (2012) Linking crystallographic model and data quality. *Science 366*, 1030−1033.
(26) Long, F., Vagin, A. A., Young, P., and Murshudov, G. N. (2008) BALBES: A molecular-replacement pipeline. *Acta Crystallogr. D64*, 125−132.
(27) Hou, J., Wojciechowska, K., Zheng, H., Chruszcz, M., Cooper, D. R., Cymborowski, M., Skarina, T., Gordon, E., Luo, H., Savchenko, A., and Minor, W. (2012) Structure of a short-chain dehydrogenase/reductase from *Bacillus anthracis*. *Acta Crystallogr. F68*, 632−637.
(28) Perrakis, A., Morris, R., and Lamzin, V. S. (1999) Automated protein model building combined with iterative structure refinement. *Nat. Struct. Biol. 6*, 458−463.
(29) Murshudov, G. N., Vagin, A. A., and Dodson, E. J. (1997) Refinement of macromolecular structures by the maximum-likelihood method. *Acta Crystallogr. D53*, 240−255.
(30) Vagin, A., and Teplyakov, A. (2010) Molecular replacement with MOLREP. *Acta Crystallogr. D66*, 22−25.
(31) Winn, M. D., Ballard, C. C., Cowtan, K. D., Dodson, E. J., Emsley, P., Evans, P. R., Keegan, R. M., Krissinel, E. B., Leslie, A. G., McCoy, A., McNicholas, S. J., Murshudov, G. N., Pannu, N. S., Potterton, E. A., Powell, H. R., Read, R. J., Vagin, A., and Wilson, K. S. (2011) Overview of the CCP4 suite and current developments. *Acta Crystallogr. D67*, 235−242.
(32) Emsley, P., Lohkamp, B., Scott, W. G., and Cowtan, K. (2010) Features and development of Coot. *Acta Crystallogr. D66*, 486−501.
(33) Schüttelkopf, A. W., and van Aalten, D. M. (2004) PRODRG: A tool for high-throughput crystallography of protein-ligand complexes. *Acta Crystallogr. D60*, 1355−1363.
(34) Chen, V. B., Arendall, W. B., III, Headd, J. J., Keedy, D. A., Immormino, R. M., Kapral, G. J., Murray, L. W., Richardson, J. S., and Richardson, D. C. (2010) MolProbity: All-atom structure validation for macromolecular crystallography. *Acta Crystallogr. D66*, 12−21.
(35) Ho, S. N., Hunt, H. D., Horton, R. M., Pullen, J. K., and Pease, L. R. (1989) Site-directed mutagenesis by overlap extension using the polymerase chain reaction. *Gene 77*, 51−59.
(36) Kallio, P., Sultana, A., Niemi, J., Mäntsälä, P., and Schneider, G. (2006) Crystal structure of the polyketide cyclase AknH with bound substrate and product analogue: Implications for catalytic mechanism and product stereoselectivity. *J. Mol. Biol. 357*, 210−220.
(37) Podschun, B., Jahnke, K., Schnackerz, K. D., and Cook, P. F. (1993) Acid base catalytic mechanism of the dihydropyrimidine dehydrogenase from pH studies. *J. Biol. Chem. 268*, 3407−3413.
(38) Persson, B., Kallberg, Y., Oppermann, U., and Jornvall, H. (2003) Coenzyme-based functional assignments of short-chain dehydrogenases/reductases (SDRs). *Chem.-Biol. Interact. 143−144*, 271−278.
(39) Krissinel, E., and Henrick, K. (2007) Inference of macromolecular assemblies from crystalline state. *J. Mol. Biol. 372*, 774−797.
(40) MacKenzie, A. K., Kershaw, N. J., Hernandez, H., Robinson, C. V., Schofield, C. J., and Andersson, I. (2007) Clavulanic acid dehydrogenase: Structural and biochemical analysis of the final step in the biosynthesis of the β-lactamase inhibitor clavulanic acid. *Biochemistry 46*, 1523−1533.
(41) Teartasin, W., Limpkin, C., Glod, F., Spencer, J., Cox, R. J., Simpson, T. J., Crosby, J., Crump, M. P., and Hadfield, A. T. (2004) Expression, purification and preliminary X-ray diffraction analysis of a ketoreductase from a type II polyketide synthase. *Acta Crystallogr. D60*, 1137−1138.
(42) Holm, L., and Rosenström, P. (2010) Dali server: Conservation mapping in 3D. *Nucleic Acids Res. 38*, W545−W549.
(43) Hadfield, A. T., Limpkin, C., Teartasin, W., Simpson, T. J., Crosby, J., and Crump, M. P. (2004) The crystal structure of the actIII actinorhodin polyketide reductase: Proposed mechanism for ACP and polyketide binding. *Structure 12*, 1865−1875.
(44) Korman, T. P., Hill, J. A., Vu, T. N., and Tsai, S. C. (2004) Structural analysis of actinorhodin polyketide ketoreductase: Cofactor binding and substrate specificity. *Biochemistry 43*, 14529−14538.
(45) Keatinge-Clay, A. T., and Stroud, R. M. (2006) The structure of a ketoreductase determines the organization of the β-carbon processing enzymes of modular polyketide synthases. *Structure 14*, 737−748.
(46) Keatinge-Clay, A. T. (2007) A tylosin ketoreductase reveals how chirality is determined in polyketides. *Chem. Biol. 14*, 898−908.
(47) Zheng, J., Taylor, C. A., Piasecki, S. K., and Keatinge-Clay, A. T. (2010) Structural and functional analysis of A-type ketoreductases from the amphotericin modular polyketide synthase. *Structure 18*, 913−922.
(48) Andersson, A., Jordan, D., Schneider, G., and Lindqvist, Y. (1996) Crystal structure of the ternary complex of 1,3,8-trihydroxynaphthalene reductase from *Magnaporthe grisea* with NADPH and an active-site inhibitor. *Structure 4*, 1161−1170.

(49) Oppermann, U., Filling, C., Hult, M., Shafqat, N., Wu, X., Lindh, M., Shafqat, J., Nordling, E., Kallberg, Y., Persson, B., and Jörnvall, H. (2003) Short-chain dehydrogenases/reductases (SDR): The 2002 update. *Chem.-Biol. Interact. 143−144*, 247−253.
(50) Filling, C., Berndt, K. D., Benach, J., Knapp, S., Prozorovski, T., Nordling, E., Ladenstein, R., Jörnvall, H., and Oppermann, U. (2002) Critical residues for structure and catalysis in short-chain dehydrogenases/reductases. *J. Biol. Chem. 277*, 25677−25684.
(51) Kavanagh, K. L., Jornvall, H., Persson, B., and Oppermann, U. (2008) Medium- and short-chain dehydrogenase/reductase gene and protein families: The SDR superfamily: Functional and structural diversity within a family of metabolic and regulatory enzymes. *Cell. Mol. Life Sci. 65*, 3895−3906.
(52) Javidpour, P., Korman, T. P., Shakya, G., and Tsai, S. C. (2011) Structural and biochemical analyses of regio- and stereospecificities observed in a type II polyketide ketoreductase. *Biochemistry 50*, 4638−4649.
(53) Caffrey, P. (2003) Conserved amino acid residues correlating with ketoreductase stereospecificity in modular polyketide synthases. *ChemBioChem 4*, 654−657.
(54) Schatz, A., Bugle, E., and Waksman, S. A. (1944) Streptomycin, a substance exhibiting antibiotic activity against Gram-positive and Gram-negative bacteria. *Exp. Biol. Med. 55*, 66−69.
(55) Lindqvist, Y., Koskiniemi, H., Jansson, A., Sandalova, T., Schnell, R., Liu, Z., Mäntsälä, P., Niemi, J., and Schneider, G. (2009) Structural basis for substrate recognition and specificity in aklavinone-11-hydroxylase from rhodomycin biosynthesis. *J. Mol. Biol. 393*, 966−977.
(56) Sciara, G., Kendrew, S. G., Miele, A. E., Marsh, N. G., Federici, L., Malatesta, F., Schimperna, G., Savino, C., and Vallone, B. (2003) The structure of ActVA-Orf6, a novel type of monooxygenase involved in actinorhodin biosynthesis. *EMBO J. 15*, 205−215.
(57) Grocholski, T., Koskiniemi, H., Lindqvist, Y., Mäntsälä, P., Niemi, J., and Schneider, G. (2010) Crystal structure of the cofactor-independent monooxygenase SnoaB from *Streptomyces nogalater*: Implications for the reaction mechanism. *Biochemistry 49*, 934−944.